

Lawrence Berkeley National Laboratory

Recent Work

Title

A NOTE ON THE CONSTRUCTION OF PROJECTION OPERATORS IN THE SEMI-CLASSICAL APPROXIMATION

Permalink

<https://escholarship.org/uc/item/1816p23v>

Author

Hahn, Yukap

Publication Date

1972-02-01

Submitted to Physical Review

LBL-718 21
Preprint

For Reference
Not to be taken from this room

A NOTE ON THE CONSTRUCTION OF PROJECTION
OPERATORS IN THE SEMI-CLASSICAL APPROXIMATION

Yukap Hahn and Kenneth M. Watson

February 9, 1972

AEC Contract No. W-7405-eng-48



DISCLAIMER

This document was prepared as an account of work sponsored by the United States Government. While this document is believed to contain correct information, neither the United States Government nor any agency thereof, nor the Regents of the University of California, nor any of their employees, makes any warranty, express or implied, or assumes any legal responsibility for the accuracy, completeness, or usefulness of any information, apparatus, product, or process disclosed, or represents that its use would not infringe privately owned rights. Reference herein to any specific commercial product, process, or service by its trade name, trademark, manufacturer, or otherwise, does not necessarily constitute or imply its endorsement, recommendation, or favoring by the United States Government or any agency thereof, or the Regents of the University of California. The views and opinions of authors expressed herein do not necessarily state or reflect those of the United States Government or any agency thereof or the Regents of the University of California.

A NOTE ON THE CONSTRUCTION OF PROJECTION
OPERATORS IN THE SEMI-CLASSICAL APPROXIMATION*

Yukap Hahn[†] and Kenneth M. Watson

Physics Department and Lawrence Berkeley Laboratory
University of California, Berkeley, California 94720

February 9, 1972

ABSTRACT

The projection operators onto various subsets of states of a quantum mechanical system are constructed in a semi-classical approximation based on the Wigner transformation of statistical mechanics. As illustrations, explicit operator expressions are derived for the cases of central Coulomb potential, one-dimensional harmonic oscillator, and the radial Coulombic states of specified angular momenta. Accuracy of these operators is then examined in some detail in terms of the overlap integrals and dipole transition probabilities. The semi-classical approximation is found to be effective in the energy regions away from the classical turning points. Extensions of the approach to partially projected Green's functions and other related moments are discussed and their applications to scattering problems pointed out.

I. INTRODUCTION

Projection operators occur frequently in formulations of theories of scattering reactions, such as that of Feshbach¹ and its subsequent developments.² For example, a calculation of compound resonance states may be set up in terms of the closed channel operator Q which is orthogonal to all open channels at a given energy E . The variational bound formulation³ of effective potentials and resulting bounds on reaction matrix elements is also developed with the use of projection operators.

The difficulty of constructing such projection operators has been an obstacle in the application of these theories. In this paper we describe the use of the Wigner⁴ transformation of statistical mechanics to provide a semi-classical approximation for projection operators.

The Wigner transformation expresses the Boltzmann function as a certain Fourier transform of the quantum mechanical density matrix. Applied to the case of the single particle distribution function this relation is⁵

$$f(\vec{x}, \vec{p}) = h^{-3} \int \left(\vec{x} - \frac{\vec{r}}{2} \middle| \rho \middle| \vec{x} + \frac{\vec{r}}{2} \right) \exp[i\vec{p} \cdot \vec{r} / \hbar] d^3r. \quad (1.1)$$

Here f is the Boltzmann function for a particle at \vec{x} with momentum \vec{p} and $(\vec{x} | \rho | \vec{x}')$ is the density matrix in a coordinate space representation.⁶ The inverse of (1.1) is

$$(\vec{x} | \rho | \vec{y}) = \int d^3p f\left(\frac{1}{2}(\vec{x} + \vec{y}), \vec{p}\right) \exp[i\vec{p} \cdot (\vec{x} - \vec{y}) / \hbar]. \quad (1.2)$$

The normalization in Eq. (1.1) is so chosen that

$$\int f(\vec{x}, \vec{p}) d^3x d^3p = \int d^3x (\vec{x} | \rho | \vec{x}) = 1 \quad (1.3)$$

when ρ is expressed in a Hilbert space representation:

$$(\vec{x}|\rho|\vec{y}) = \frac{1}{M} \sum_{\alpha=1}^M \psi_{\alpha}(\vec{x}) \psi_{\alpha}^{\dagger}(\vec{y}), \quad (1.4)$$

the average being over an appropriate ensemble with ψ_{α} the wave function of α in that ensemble.

II. PROJECTION OPERATOR ONTO STATES OF ONE OR MORE PARTICLES

Relations (1.1), (1.2), and (1.4) suggest the application to projection operator construction with a change in normalization, of course. Consider a complete set $\chi_{\lambda}(\vec{x})$ of orthonormal single particle wave function. The projection operator onto a subset \mathcal{S} of these is

$$(\vec{x}|\Lambda|\vec{y}) = \sum_{\mathcal{S}} \chi_{\lambda}(\vec{x}) \chi_{\lambda}^*(\vec{y}). \quad (2.1)$$

A classical phase space function $F(\vec{x}, \vec{p})$ is introduced as⁷

$$F(\vec{x}, \vec{p}) = \int \left(\vec{x} - \frac{\vec{r}}{2} | \Lambda | \vec{x} + \frac{\vec{r}}{2} \right) \exp[i\vec{p} \cdot \vec{r} / \hbar] d^3r. \quad (2.2)$$

The inverse transformation is

$$(\vec{x}|\Lambda|\vec{y}) = \frac{1}{h^3} \int F\left(\frac{1}{2}(\vec{x} + \vec{y}), \vec{p}\right) \exp\left[i\frac{\vec{p}}{\hbar} \cdot (\vec{x} - \vec{y})\right] d^3p. \quad (2.3)$$

If the χ_{λ} are normalized to unity, the normalization of F is

$$\int F(\vec{x}, \vec{p}) d^3x d^3p = h^3 \sum_{\mathcal{S}}. \quad (2.4)$$

Consider now the plane wave states

$$\chi_{\frac{\vec{p}}{P}}(\vec{x}) = h^{-\frac{3}{2}} \exp[i\vec{p} \cdot \vec{x} / \hbar]$$

in some large volume \mathcal{V} . The projection operator onto states of momentum less than P is

$$(\vec{x}|\Lambda|\vec{y}) = h^{-3} \int_{p < P} d^3p \exp[i(\vec{x} - \vec{y}) \cdot \vec{p} / \hbar]. \quad (2.5)$$

For this projection operator Eq. (2.2) gives

$$F(\vec{x}, \vec{p}) = \int_{q < P} d^3q \delta(\vec{q} - \vec{p}), \quad \vec{x} \text{ in } \mathcal{V}. \quad (2.6)$$

We see that F is unity in the "allowed" region ($p < P$) of phase space and vanishes outside this region.

The above suggests the following approximate model for a projection operator. Define

$$F(\vec{x}, \vec{p}) = 1,$$

with (\vec{x}, \vec{p}) in a region \mathcal{R} of classical phase space, and

$$F(\vec{x}, \vec{p}) = 0, \quad (\vec{x}, \vec{p}) \text{ not in } \mathcal{R}. \quad (2.7)$$

Then the quantum mechanical projection operator corresponding to the classical phase space \mathcal{R} is

$$\begin{aligned} (\vec{x} | \Lambda | \vec{y}) &= h^{-3} \int d^3p \exp[i\vec{p} \cdot (\vec{x} - \vec{y})/\hbar], \\ &\text{with } ((\frac{1}{2}(\vec{x} + \vec{y}), \vec{p}) \text{ in } \mathcal{R}). \end{aligned} \quad (2.8)$$

The generalization to the case of N particles is obvious.

Let $F(\vec{x}_1, \vec{p}_1, \dots, \vec{x}_N, \vec{p}_N)$ be unity in a region \mathcal{R} of the N -particle phase space and let F vanish outside this region. Then the corresponding projection operator is

$$\begin{aligned} (\vec{x}_1, \dots, \vec{x}_N | \Lambda | \vec{y}_1, \dots, \vec{y}_N) &= h^{-3N} \int d^3p_1 \dots d^3p_N F \\ &\times \exp \left[i \sum_{j=1}^N \vec{p}_j \cdot (\vec{x}_j - \vec{y}_j) / \hbar \right]. \end{aligned} \quad (2.9)$$

The case of a particle in a spherically symmetric attractive potential $V(r)$ is very simple. Suppose $V(r)$ approaches zero as $r \rightarrow \infty$. Then choose

$$\begin{aligned} F(\vec{x}, \vec{p}) &= 1 \text{ for } \frac{p^2}{2m} + V(r) \leq E \leq 0, \\ &= 0 \text{ otherwise.} \end{aligned} \quad (2.10)$$

Let

$$P(x) = [2m(E - V(x))]^{\frac{1}{2}}. \quad (2.11)$$

[We are to set $P = 0$ if the right-hand side of (2.11) is imaginary.]

The expression (2.8) then gives us

$$(\vec{x} | \Lambda | \vec{y}) = \frac{1}{2\pi^2 |\vec{x} - \vec{y}|^3} [\sin G - G \cos G],$$

$$G = [|\vec{x} - \vec{y}| P(\frac{1}{2}|\vec{x} + \vec{y}|)] / \hbar. \quad (2.12)$$

The projection operator onto all bound states of a Coulomb potential, for example,

$$V(r) = -Ze^2/r$$

is then [now $E = 0$ in Eq. (2.11)]

$$\begin{aligned} (\vec{x} | \Lambda_B | \vec{y}) &= \left[2\pi^2 (a_0 |\vec{x} + \vec{y}| / (4Z)) \right]^{\frac{3}{2}-1} \\ &\times [\sin G/G^3 - \cos G/G^2], \end{aligned}$$

$$G = |\vec{x} - \vec{y}| \left[\frac{4Z}{a_0 |\vec{x} + \vec{y}|} \right]^{\frac{1}{2}}, \quad (2.13)$$

where a_0 is the Bohr radius.

The projection operator onto the continuum of the Coulomb states is, in the present approximation, obtained as follows:

$$F_C = 1 - F,$$

so

$$(\vec{x} | \Lambda_C | \vec{y}) = \delta(\vec{x} - \vec{y}) - (\vec{x} | \Lambda_B | \vec{y}). \quad (2.14)$$

The relation (2.14) is of course exact. This results from the fact that if $F = 1$ on all phase space our approximation gives the exact result

$$(\vec{x}|\Lambda|\vec{y}) = \delta(\vec{x} - \vec{y}) . \quad (2.15)$$

We emphasize that the expressions (2.12) and (2.13) are defined only in that domain of \vec{x} and \vec{y} for which $P((\vec{x} + \vec{y})/2)$ is real. Thus $(\vec{x}|\Lambda|\vec{y})$ vanishes for $(\vec{x} + \vec{y})/2$ outside the classical turning points. Extension of our procedure into the classically forbidden regime appears possible (as in the WKB method), but is not discussed here.

The formal relation

$$\Lambda^2 = \Lambda \quad (2.16)$$

to be satisfied by projection operators is not satisfied exactly by the approximation (2.8). As the domain \mathcal{R} becomes large compared with \hbar^3 --the semi-classical limit--it is easily seen that (2.16) becomes valid, however. For the classical phase space \mathcal{R} described by the symmetric variable $(\vec{x} + \vec{y})/2$, the operator given by (2.8) is hermitian.

The expression corresponding to (2.3) when a momentum space representation is used is

$$\begin{aligned} (\vec{q}|\hat{\Lambda}|\vec{q}') &= \hbar^{-3} \int d^3x d^3y \exp[i(\vec{q}' \cdot \vec{y} - \vec{q} \cdot \vec{x})](\vec{x}|\Lambda|\vec{y}) \\ &= \hbar^{-3} \int d^3r F(\vec{r}, (\vec{q} + \vec{q}')/2) \exp[i(\vec{q}' - \vec{q}) \cdot \vec{r}] . \end{aligned} \quad (2.17)$$

It is also of interest to consider the applications of (2.5) and (2.9) to collision problems. For scatterings in which all the states in the set \mathcal{S} correspond to open channels, Λ_B for the

states in \mathcal{S} may be used to construct the open-channel projection operators. Thus, for example, in the e-H scattering near the ionization threshold, we may use $\Lambda_B(\vec{I}; \vec{I}')$ of (2.12) and construct the operator as

$$\begin{aligned} \Lambda_B(\vec{I}, \vec{z}; \vec{I}', \vec{z}') &= \Lambda_B(\vec{I}; \vec{I}') + \Lambda_B(\vec{z}; \vec{z}') \\ &- \Lambda_B(\vec{I}; \vec{I}') \Lambda_B(\vec{z}; \vec{z}') \equiv \Lambda^P \end{aligned} \quad (2.18)$$

and its complement

$$\Lambda_C(\vec{I}, \vec{z}; \vec{I}', \vec{z}') = \delta(\vec{I} - \vec{I}') \delta(\vec{z} - \vec{z}') - \Lambda_B(\vec{I}, \vec{z}; \vec{I}', \vec{z}') \equiv \Lambda^Q, \quad (2.19)$$

where $[\Lambda_B(\vec{I}, \vec{I}'), \Lambda_B(\vec{z}; \vec{z}')] = 0$. These operators, which are hermitian and almost idempotent, may then be used to study the resonance structure, distortion effect, and the bounds on scattering parameters³ near the ionization threshold. Alternatively, a similar projection operator Λ^Q onto the closed-channel space \mathcal{Q} for the two-electron system may also be obtained directly from the multiparticle generalization (2.9). The effective pseudopotential for this process can then be constructed with Λ^Q .

Generalizations of (2.18) and (2.19) to systems involving more than two electrons are also straightforward and the result could be used with greater advantage in the e-Atomic and e-Molecular reactions, simply because Λ^P and Λ^Q are now very simple to evaluate.

III. APPLICATIONS OF COULOMB PROJECTION OPERATOR

As a first application of the projection operators derived in Sec. II, we study the ionization transitions of hydrogenic targets by fast electron impact.⁸ Since the bound state \rightarrow bound state transitions are dominant in this case, the usual closure approximation to the transition probabilities leads to gross overestimate, and it is necessary to carefully isolate the continuum contributions. Thus, the relevant transition probability is given in the leading order by

$$M_{nl}^C = \frac{1}{2\ell + 1} \sum_m \langle n, \ell, m; \vec{x} | \vec{x} \cdot \Lambda_C(\vec{x}, \vec{y}) \vec{y} | n, \ell, m; \vec{y} \rangle, \quad (3.1)$$

where all the dipole transitions from $|n, \ell, m; \vec{x}\rangle$ to the continuum are included. Similarly, we also have

$$M_{nl}^B = \frac{1}{2\ell + 1} \sum_m \langle n, \ell, m; \vec{x} | \vec{x} \cdot \Lambda_B(\vec{x}, \vec{y}) \vec{y} | n, \ell, m; \vec{y} \rangle \quad (3.2)$$

corresponding to the transitions to all the bound states.

In (3.1) and (3.2), we have denoted the hydrogenic states as

$$|n, \ell, m; \vec{x}\rangle \equiv \psi_{n\ell m}(\vec{x}) = R_{n\ell}(x) Y_{\ell m}(\hat{x}), \quad (3.3)$$

while the projection operators Λ_B and Λ_C are given by (2.13) and (2.14), with $E = 0$.

Evidently, the contribution to (3.1) coming from the δ -function part in (2.14) corresponds to transitions to all available states, both bound and continuum, and is given in this case by⁹

$$\begin{aligned} \bar{M}_{nl}^A &= \frac{1}{2\ell + 1} \sum_m \langle n, \ell, m; \vec{x} | \vec{x} \cdot \delta(\vec{x} - \vec{y}) \vec{y} | n, \ell, m; \vec{y} \rangle \\ &= \bar{M}_{nl}^B + \bar{M}_{nl}^C \\ &= \frac{1}{2} [5n^2 + 1 - 3\ell(\ell + 1)], \end{aligned} \quad (3.4)$$

where the quantities defined with bar denote exact values. An additional quantity of interest for our study is the overlap integral defined as

$$S_{nl} = \frac{1}{2\ell + 1} \sum_m \langle n, \ell, m; \vec{x} | \Lambda_B(\vec{x}, \vec{y}) | n, \ell, m; \vec{y} \rangle. \quad (3.5)$$

Obviously, with the exact $\bar{\Lambda}_B$ in (3.5), in place of the approximate form (2.13), we expect that

$$\begin{aligned} \bar{S}_{nl} &= 1, \text{ for the } n\text{th state in } \bar{\Lambda}_B \\ &= 0 \text{ otherwise.} \end{aligned} \quad (3.6)$$

The exact values of \bar{M}_{nl}^B and \bar{M}_{nl}^C are also available⁹ for $n \leq 4$ for ready comparison.

More explicitly, after the sum over the magnetic quantum numbers is carried out, M_{nl}^B becomes

$$\begin{aligned} M_{nl}^B &= \frac{1}{\pi} \int_0^\infty x^2 dx \int_0^\infty y^2 dy R_{n\ell}(x) R_{n\ell}(y) \int_{-1}^1 d\mu P_\ell(\mu) \mu \\ &\quad \times \left[\frac{\sin G - G \cos G}{u^3} \right]. \end{aligned} \quad (3.7)$$

For some values of μ in the range $|\mu| \leq 1$, the variable v goes through zeros and thus G becomes singular. This causes the integrand

in (3.9) to oscillate violently and makes the du integration difficult. To avoid this problem in the actual numerical integration, we change the variables (\vec{x}, \vec{y}) to (\vec{x}, \vec{t}) , where $\vec{t} \equiv \vec{x} + \vec{y}$, and rewrite the M_{nl}^B in the form

$$M_{nl}^B = \frac{1}{\pi} \int_0^\infty x^2 dx \int_0^\infty t^2 dt R_{nl}(x) \int_{-1}^1 R_{nl}(b) \frac{1}{d^3} [\sin G - G \cos G] \times (t\alpha - x) P_\ell(\mu) d\alpha, \quad (3.8)$$

where

$$\begin{aligned} d &= [4x^2 + t^2 - 4xt\alpha]^{\frac{1}{2}} \\ b &= [t^2 + x^2 - 2xt\alpha]^{\frac{1}{2}} \\ G &= 2d/(t)^{\frac{1}{2}} \\ \mu &= (t\alpha - x)/b. \end{aligned} \quad (3.9)$$

The form (3.8) and the corresponding expression for S_{nl} were used in the actual numerical calculations, and the result is given in Table I for the cases $n = 1, 2, 3$ and $\ell = 0$. A semianalytic integration formula, which is useful for rapidly oscillating integrands, and the Newton-Cotes five-point formulas with varying mesh sizes are used to ascertain the accuracy of the triple integrations in (3.8). The actual values given in the table are obtained by rough extrapolations to the limit of zero mesh sizes (Fig. 1). The mesh size h is defined here by $h = 2/K_{\max}$; the convergence was found to be extremely slow, and becomes worse as n was increased, especially in the $d\alpha$ integration of (3.8).

We have encountered additional difficulties in the evaluation of M_{nl}^C , because of the severe cancellation between M_{nl}^A and M_{nl}^B for $n > 1$, where $M_{nl}^A \approx M_{nl}^B \gg M_{nl}^C$. This seems to be a peculiarity of the Coulomb problem under consideration. The difficulty could in principle be avoided by defining Λ_C directly in a form similar to (2.8), rather than through Λ_B as we have done in (2.14). When the order of integrations d^3p and du are interchanged, the resulting integral is then well-defined. However, we are left with four dimensional integrations which are difficult to carry out numerically. For the case $n = 1$ and $\ell = 0$, we obtain $M_{10}^C \approx 1.1 \pm 0.2$.

IV. PROJECTION OPERATOR IN ONE-DIMENSION (HARMONIC OSCILLATOR)

We consider in this section a one-dimensional harmonic oscillator model. Aside from the simplification in the numerical analysis, the model involves a very simple dipole coupling scheme and also allows us to study the accuracy of Λ_B near the classical turning point.

The parameters of the model are defined in the units $m = \hbar = 1$, by¹⁰

$$\frac{d^2 \phi_n}{dx^2} + a^2 x^2 \phi_n = E_n \phi_n \quad (4.1)$$

with

$$E_n = (2n + 1)a, \quad n = 0, 1, 2, \dots \quad (4.2)$$

$$\phi_n(x) = \Lambda_n H_n[(a)^{1/2}x] \exp(-\frac{1}{2}ax^2)$$

and

$$\int_{-\infty}^{\infty} |\phi_n(x)|^2 dx = 1.$$

The dipole coupling produces

$$\left[\int_{-\infty}^{\infty} \phi_n^*(x) x \phi_m(x) dx \right]^2 = \begin{cases} \frac{n+1}{2a} \equiv \bar{M}_{n,n+1}, & \text{for } m = n+1 \\ \frac{n}{2a} \equiv \bar{M}_{n,n-1}, & \text{for } m = n-1 \\ 0, & \text{otherwise.} \end{cases} \quad (4.3)$$

We let

$$\bar{M}_n = \bar{M}_{n,n+1} + \bar{M}_{n,n-1} = \frac{2n+1}{2a}. \quad (4.4)$$

The operator $\bar{\Lambda}_B$ which projects onto all the states with energy $E_n \leq E_C$ is

$$(x|\bar{\Lambda}_B|y) = \sum_{E_n \leq E_C} \phi_n(x) \phi_n^*(y). \quad (4.5)$$

The one-dimensional analogue of (2.8) gives us the semi-classical approximation to (4.5)

$$\begin{aligned} (x|\Lambda_B|y) &= \frac{1}{2\pi} \int_{-P}^P dp e^{ip(x-y)} \\ &= \frac{1}{\pi} \frac{\sin(Pu)}{u}. \end{aligned} \quad (4.6)$$

Here

$$P^2(v) = 2E_C - a^2 v^2. \quad (4.7)$$

and

$$u = x - y, \quad v = (x + y)/2. \quad (4.8)$$

In addition to (4.6) we define

$$\begin{aligned} (x|\Lambda_B^\pm|y) &= \begin{cases} \frac{1}{2\pi} \int_0^P dp \cos(px) \cos(py), & \text{even} \\ \frac{1}{2\pi} \int_0^P dp \sin(px) \sin(py), & \text{odd} \end{cases} \\ &= \frac{1}{2\pi} [\sin(Pu)/u \pm \sin(2Pv)/(2v)]. \end{aligned} \quad (4.9)$$

00303707/86

We note that Λ_B and Λ_B^\pm vanish for $|v| > v_C$, where

$$v_C \equiv (2E_C/a)^{\frac{1}{2}}. \quad (4.10)$$

The quantities Λ_B^\pm would represent projection operators onto even (odd) states, corresponding to even (odd) n-values, except for the wrong symmetry of Eqs. (4.7) and (4.8). We shall see, however, that for those cases considered below Λ_B^\pm represent very good approximations to the projection operators on even (odd) states.

The quantities of interest are defined by

$$M_n^A = (n, x | x^2 | n, x) \quad (4.11)$$

$$M_n^B = (n, x | x \Lambda_B y | n, y) \quad (4.12)$$

$$M_n^C = M_n^A - M_n^B \quad (4.13)$$

$$S_n = (n, x | \Lambda_B | n, y) \quad (4.14)$$

and the corresponding integrals with Λ_B^\pm in the place of Λ_B . We denote them by $M_n^{B\pm}$, $M_n^{C\pm}$, and S_n^\pm .

The dipole couple scheme of this model is very simple, and we have the exact values for comparison

$$\bar{M}_n^A = \bar{M}_n^B \quad (4.15)$$

$$\bar{M}_n^C = 0 \quad (4.16)$$

and

$$\bar{S}_n^\pm = 1 \text{ or } 0, \text{ depending on the symmetry of } n \text{ and } \Lambda_B^\pm$$

$$\bar{S}_n = 1.$$

The parameters of the model are chosen as

$$a^2 = 0.45 \quad (4.17)$$

$$2E_C = 2n_C + 1, \text{ with } n_C = 10,$$

which in turn gives the cutoff value

$$v_C = \left[\frac{2n_C + 1}{a} \right]^{\frac{1}{2}} \approx 5.6. \quad (4.18)$$

Table II contains the result of calculation for both cases in which Λ_B and Λ_B^\pm are used. The extra term in Λ_B^\pm causes both $M_n^{B\pm}$ and S_n^\pm to oscillate around their respective exact values, while the integrals with Λ_B give smoother variations in n. The deviations of M_n^B , S_n , $M_n^{B\pm}$, and S_n^\pm are illustrated in Figs. 2 and 3. Also included in Table II is the overlap integral \tilde{S}_n^\pm which was calculated using the wrong symmetry, that is, Λ_B^\pm for the case with n odd, and vice versa. Although the form of integrands in (4.9) are either symmetric or antisymmetric under $x \rightarrow -x$ (or $y \rightarrow -y$), Λ_B^\pm itself does not have the definite symmetry because of the cutoff (4.10). However, we expect that $\tilde{S}_n^\pm \approx 0$ for those n which are away from n_C , as given in the table. In fact, we have $\tilde{S}_n^\pm = S_n - S_n^\pm$, and the exact value would of course be $\tilde{S}_n^\pm = 0$.

The quantity (3.2) can be reduced to the form, by performing the angular integrations,

$$M_{nl}^B = [(2l+1)]^{-1} \int_0^\infty x^3 dx \int_0^\infty y^3 dy$$

$$\times R_{nl}(x) R_{nl}(y) [\ell(x|\Lambda_B^{\ell-1}|y) + (\ell+1)(x|\Lambda_B^{\ell+1}|y)]$$

$$= [(2l+1)]^{-1} [\ell M_{nl-}^B + (\ell+1) M_{nl+}^B]. \quad (5.10)$$

The corresponding quantity $M_{nl\pm}^C$ is

$$M_{nl\pm}^C = M_{nl}^A - M_{nl\pm}^B, \quad (5.11)$$

where M_{nl}^A is given by Eq. (3.6). In general, $M_{nl+}^C \gg M_{nl-}^C$, so that we have $M_{nl}^C \approx M_{nl+}^C$. Finally, the normalization integral S_{nl} , defined by Eq. (3.7), is

$$S_{nl} = \int_0^\infty x^2 dx \int_0^\infty y^2 dy R_{nl}(x) R_{nl}(y) (x|\Lambda_B^\ell|y). \quad (5.12)$$

We can also define analogous quantities using the approximation (5.9) and Λ_{BO}^ℓ , and denote them as $M_{nl\pm}^{BO}$, $S_{nl\pm}^O$, $M_{nl\pm}^{CO}$, etc.

As is clear from the above discussion, there are essentially two ambiguities in the present case; we could choose either (5.8a) or (5.8b) for the value of L^2 and thus the cutoff v_C , and secondly we could use either (5.7) or (5.9) for Λ_B (and Λ_{BO}). We have considered here all four possibilities. Table III contains the result of calculations with $L^2 \approx L_C^2 = (\ell + \frac{1}{2})^2$ and both $\Lambda_{BO}^{\ell+1}$ and $\Lambda_B^{\ell+1}$. We thus have M_{nl+}^{BO} , M_{nl+}^B , and M_{nl+}^{CO} , and M_{nl+}^C corresponding to the

transitions $\ell \rightarrow \ell + 1$. The cases with $L^2 \approx L_Q^2 = \ell(\ell+1)$ are considered in Table IV.

First of all, we should point out that, as in the three-dimensional Coulomb case studied in Sec. III, $M_{nl}^A \gtrsim M_{nl}^B \gg M_{nl}^C$ (Fig. 4). Therefore the accuracy of Λ_B and Λ_{BO} should be judged in terms of S_{nl} and M_{nl}^B , rather than by looking at the small M_{nl}^C . Secondly, the results in Tables III and IV are not very sensitive to the choices of L^2 , so long as it is chosen judiciously. Incidentally, the cutoff for $v < v_C$ partially corrects for the error caused by the use of asymptotic j_ℓ in (5.7). Finally, we note that the extra term in Λ_B (i.e., $\Lambda_B - \Lambda_{BO}$) gives rise to small oscillations in M_{nl+}^C , while Λ_{BO} yields fairly smooth M_{nl+}^{CO} .

VI. APPROXIMATION TO GREEN'S FUNCTIONS

The reasonable accuracy of the semi-classical approximation for projection operators suggests a similar application to certain other operators. In the present section we discuss the construction of partially projected Green's functions by this technique.

We introduce the "Green's function"

$$(\vec{x}|\bar{G}_B|\vec{y}) = \sum_{\mathcal{S}} \chi_{\lambda}(\vec{x})(E - E_{\lambda})^{-1} \chi_{\lambda}^*(\vec{y}). \quad (6.1)$$

Here the E_{λ} are eigenvalues of the energy for states χ_{λ} , members of a complete orthonormal set $\{\chi_{\lambda}\}$, and the sum extends over a subset \mathcal{S} of these.

The semi-classical approximation to (6.1) may be obtained in exactly the same way as with (2.8) and (2.12). Thus, for all states with $E_{\lambda} \leq E_c$ and potential $V(x)$, we define

$$P(v) = [2m(E_c - V(v))]^{\frac{1}{2}} \quad (6.2)$$

and

$$E_{\lambda} \rightarrow \frac{p^2}{2m} + V(v), \quad (6.3)$$

where $\vec{v} \equiv \frac{1}{2}(\vec{x} + \vec{y})$ as before. Then, the operator \bar{G}_B in the semi-classical approximation is given by

$$(\vec{x}|\bar{G}_B|\vec{y}) = \frac{1}{h^3} \int_{p \leq P} d^3p \frac{e^{i\vec{p} \cdot \vec{u} / \hbar}}{\left(E_c - \frac{p^2}{2m} - V(v)\right)}, \quad (6.4)$$

where $\vec{u} \equiv \vec{x} - \vec{y}$. After the angular integrations, (6.4) becomes

$$(m = \hbar = e^2 = 1)$$

$$(\vec{x}|\bar{G}_B|\vec{y}) = \frac{1}{\pi^2 u} \int_0^{P(v)} \frac{p \, dp \, \sin(pu)}{2E_c - p^2 - 2V(v)}, \quad (6.5)$$

which is the desired result. Analogously, the operator in the complementary space $\bar{\mathcal{S}} = 1 - \mathcal{S}$ can also be given directly this time as

$$(\vec{x}|\bar{G}_C|\vec{y}) = \frac{1}{\pi^2 u} \int_{P(v)}^{\infty} \frac{p \, dp \, \sin(pu)}{2E_c - p^2 - 2V(v)}, \quad (6.6)$$

which should be convergent at large p because of the Riemann-Lebeque theorem. Of course, both \bar{G}_B and \bar{G}_C are defined only in the region of v such that $P(v)$ is real.

Generalizations of (6.5) and (6.6) to operators of higher moments are obvious, as

$$(\vec{x}|\bar{G}_B^{\gamma}|\vec{y}) = \frac{2^{\gamma-1}}{\pi^2 u} \int_0^{P(v)} \frac{p \, dp \, \sin(pu)}{[2E_c - p^2 - 2V(v)]^{\gamma}}, \quad \gamma \geq 0, \quad (6.7)$$

and the corresponding expression for \bar{G}_C^{γ} .

There are many possible applications of the operators (6.7); for example, the adiabatic dipole and higher multipole polarizabilities α_{ℓ} may be evaluated¹¹ using (6.5), while the leading nonadiabatic corrections β_{ℓ} to the adiabatic pseudopotentials in the low energy electron-atom collisions involve operators with $\gamma = 2$. The low-energy scattering parameters are known to be determined principally by these parameters.

The form (6.7) immediately suggests that the case with $\gamma < 0$ may also be of interest, although special care is required in the

00003701188

direct evaluation of G_C^r because of the convergence difficulties at large values of p . Thus, we have

$$(\vec{x}|F_B^\delta|\vec{y}) = \frac{1}{\pi^2 u(2)^{\delta+1}} \int_0^{P(v)} p dp \sin(pu)[2E - p^2 - 2\bar{v}]^\delta. \quad (6.8)$$

The case with $\delta = 1$ may be used, for example, in the calculation of the partially projected oscillator strength. The main advantage of dealing with the operators in the restricted set \mathcal{S} or $\bar{\mathcal{S}}$ is that the contributions from each state in that set are all of the same sign, often resulting in some type of bound property.

Some insight into the nature of the approximation (6.4) can be obtained by using it to construct the actual Green's function, G^+ , obtained by setting $P = \infty$ and using the proper retarded boundary condition.¹² This gives

$$(\vec{x}|G^+|\vec{y}) = -[M/(2\pi u)] \exp[iuK(v)], \quad (6.9)$$

where

$$K(v) = [2M(E - V(v))]^{\frac{1}{2}}. \quad (6.10)$$

The corresponding expression for G^{+13} in the straight-line eikonal approximation, [which is certainly more accurate than (6.9)] is

$$(\vec{x}|G^+|\vec{y}) = -[M/(2\pi u)] \exp \left[i \int_{\vec{y}}^{\vec{x}} K(r) ds(\vec{r}) \right]. \quad (6.11)$$

Here the path integral is taken on the straight line joining points \vec{y} and \vec{x} .

We see that (6.9) corresponds to approximating the eikonal integral as

$$\int_{\vec{y}}^{\vec{x}} K(r) ds(\vec{r}) \approx |\vec{x} - \vec{y}| K(|\vec{x} + \vec{y}|/2). \quad (6.12)$$

FOOTNOTES AND REFERENCES

* Research supported in part by the U. S. Atomic Energy Commission and by the Air Force Office of Scientific Research, Office of Aerospace Research, United States Air Force, under Contract #F44620-70-C-0028.

† On sabbatical leave from the Physics Department, University of Connecticut, Storrs, Connecticut 06268. Participating guest Lawrence Berkeley Laboratory.

1. H. Feshbach, Ann. Phys. (N.Y.) 19, 287 (1962) and 5, 357 (1958).
2. W. A. Friedman and H. Feshbach, Contribution to Racah memorial volume; M. H. Mittleman, Ann. Phys. (N.Y.) 28, 430 (1964); J. C. Y. Chen and M. H. Mittleman, *ibid* 37, 264 (1966); M. Coz, *ibid* 35, 53 (1965) and 36, 217 (1966); Y. Hahn, *ibid* 58, 137 (1970) and 67, 389 (1971).
3. Y. Hahn and L. Spruch, Phys. Rev. 153, 1159 (1967); Y. Hahn, *ibid* C1, 12 (1970).
4. E. P. Wigner, Phys. Rev. 40, 749 (1932).
5. A similar expression is of course available for the case of more than one particle [see Ref. 4].
6. See, for example, R. Balescu, Statistical Mechanics of Charged Particles (Interscience Publishers, N.Y., 1963), Chapter 14.
7. Planck's constant is retained in this section to explicitly exhibit classical and quantum aspects of our formulation.
8. See, for example, N. F. Mott and H. S. W. Massey, The Theory of Atomic Collisions (Oxford Press, 1965), Chapter 16.
9. H. A. Bethe and E. E. Salpeter, Handbuch der Physik, edited by S. Flügge (Springer-Verlag, Berlin, 1957), Vol. 35.

10. L. I. Schiff, Quantum Mechanics (McGraw-Hill Book Co. Inc., N. Y., 1955).
11. C. J. Kleinman, Y. Hahn, and L. Spruch, Phys. Rev. 165, 53 (1968).
12. M. L. Goldberger and K. M. Watson, Collision Theory (John Wiley and Sons, Inc., New York, 1964), page 303.
13. Ref. 12, page 331.

0000070189

Table I. The dipole transition probabilities and the overlap integrals for the hydrogenic system, with $n = 1, 2, 3$ and $\ell = 0$. The full projection operator Λ_B for all bound partial wave states is used. The quantities with bar denote the exact values, in atomic units.

n	\bar{M}_{n0}			M_{n0}			S_{n0}
	A	B	C	A	B	C	
1	3.00	2.15	0.85	3.00	2.07 ± 0.01	0.93 ± 0.01	0.87 ± 0.02
2	42.00	39.30	2.70	42.00	39.6 ± 0.1	2.4 ± 0.1	0.95 ± 0.02
3	207.00	202.56	4.44	207.00	189 ± 6	18 ± 6	

Table II. The dipole transition probabilities M_n and the overlap integrals S_n for the one-dimensional harmonic oscillator model. The force constant $a^2 = 0.45$ and the cutoff energy is chosen the 10th level, with $n_C = 10$. Both cases with Λ_B and Λ_B^\pm are considered.

n	Exact $\bar{M}_n^A = \bar{M}_n^B$	Λ_B			Λ_B^\pm			
		S_n	M_n^B	M_n^C	S_n^\pm	$M_n^{B\pm}$	$M_n^{C\pm}$	\tilde{S}_n^\pm
0	1.1111	1.0000	1.1111	0.0000	1.0000	1.1112	-0.0001	0.0000
1	3.3333	1.0000	3.3333	0.0000	1.0002	3.3323	0.0011	0.0000
2	5.5556	1.0000	5.5556	0.0000	0.9996	5.5593	-0.0038	0.0004
3	7.7778	1.0000	7.7774	0.0004	1.0007	7.8052	-0.0274	-0.0002
4	10.0000	1.0000	9.9968	0.0032	1.0074	9.7765	0.2235	-0.0074
5	12.2222	0.9994	12.2011	0.0212	0.9717	12.7276	-0.5054	0.0287
6	14.4444	0.9969	14.3345	0.1100	1.0196	14.070	0.374	-0.0227
7	16.6667	0.9952	16.2100	0.4566	1.0197	16.361	0.305	-0.0315
8	18.8889	0.9513	17.352	1.537	0.9931	17.945	0.944	-0.0418
9	21.1111	0.8584	16.884	4.227	0.9159	18.86	2.26	-0.0541
10	23.3333	0.6632	13.807	9.527	0.7678	18.69	4.64	-0.105

Table III. The hydrogenic dipole transition probabilities and overlap integrals using the radial projection operators Λ_{BO+}^l and Λ_{B+}^l for the case $l \rightarrow l + 1$. The choice $L^2 \approx L_C^2 \equiv (l + \frac{1}{2})^2$ is used in the cutoff v_C and momentum $P(v)$.

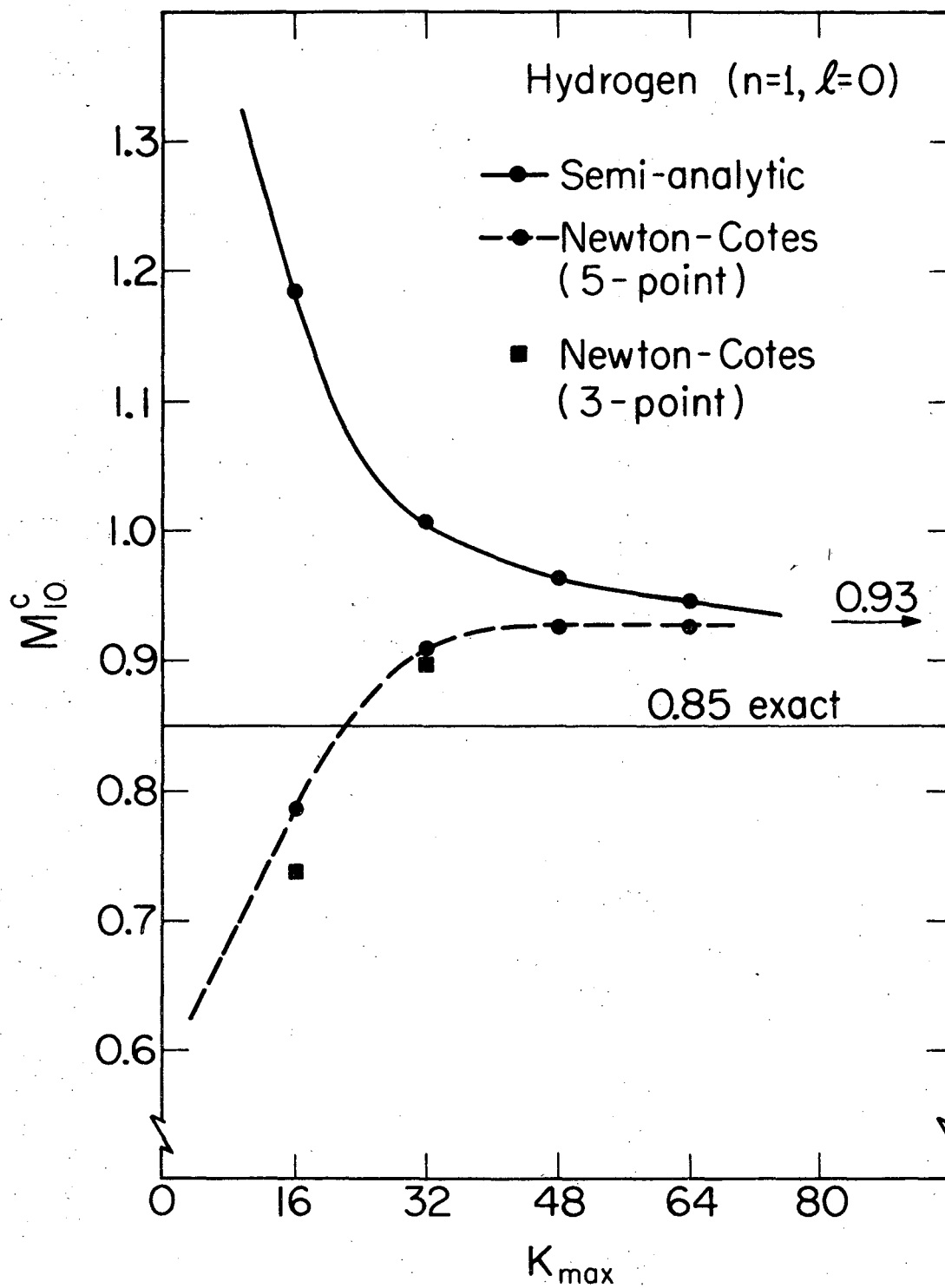
n l	Exact Values			Λ_{BO+}, L_C^2			Λ_{B+}, L_C^2		
	\bar{M}_{nl}^A	\bar{M}_{nl+}^B	\bar{M}_{nl+}^C	S_{nl}	M_{nl+}^{BO}	M_{nl+}^{CO}	S_{nl}	M_{nl+}^B	M_{nl+}^C
1 0	3.00	2.15	0.85	0.917	2.24	0.76	0.910	2.20	0.80
2 0	42.00	39.30	2.70	0.959	40.90	1.10	0.825	44.3	-2.3
3 0	207.00	202.56	4.44	0.972	205.59	1.41	1.059	190.4	16.6
4 0	648.0	642.7	5.3	0.979	646.5	1.5	0.943	668.9	-20.9
5 0	1575			0.983	1573.4	1.6	0.972	1581.5	-6.5
6 0	3255			0.985	3252.2	2.8	1.021	3151.5	103.5
2 1	30.00	27.62	2.38	0.965	26.52	3.48	0.890	27.6	2.4
3 1	180.00	174.54	5.46	0.980	176.7	3.3	0.899	181.6	-1.6
4 1	600.0	591.7	8.3	0.987	596.4	3.6	1.063	564.5	35.5
5 1	1500			0.990	1496.2	3.8	0.982	1536	-36
6 1	3148			0.991	3142.5	5.5	0.974	3174	-26

Table IV. The hydrogenic dipole transition probabilities and overlap integrals using the radial projection operators Λ_{BO+} and Λ_{B+}^l for the case $l \rightarrow l + 1$. The choice $L^2 \approx L_Q^2 \equiv l(l + 1)$ is used in the cutoff v_C and momentum $P(v)$.

n l	Exact Values			Λ_{BO+}, L_Q^2			Λ_{B+}, L_Q^2		
	\bar{M}_{nl}^A	\bar{M}_{nl+}^B	\bar{M}_{nl+}^C	S_{nl}	M_{nl+}^{BO}	M_{nl+}^{CO}	S_{nl}	M_{nl+}^B	M_{nl+}^C
1 0	3.00	2.15	0.85	0.947	2.35	0.65	0.981	2.26	0.74
2 0	42.00	39.30	2.70	0.968	41.02	0.98	0.829	44.66	-2.66
3 0	207.00	202.56	4.44	0.977	205.74	1.26	1.062	190.62	16.38
4 0	648.00	642.7	5.3	0.981	646.7	1.3	0.948	668.1	-20.1
5 0	1575			0.984	1573.6	1.4	0.972	1584.0	-9.0
6 0	3255			0.986	3252.5	2.5	1.023	3149	106
2 1	30.00	27.62	2.38	0.973	26.85	3.15	0.899	27.85	2.15
3 1	180.00	174.54	5.46	0.984	176.93	3.07	0.895	182.5	-2.5
4 1	600.0	591.7	8.3	0.990	596.7	3.3	1.062	564.6	35.4
5 1	1500			0.992	1496.5	3.5	0.985	1535	-35
6 1	3148			0.992	3142.8	5.2	0.974	3177	-29

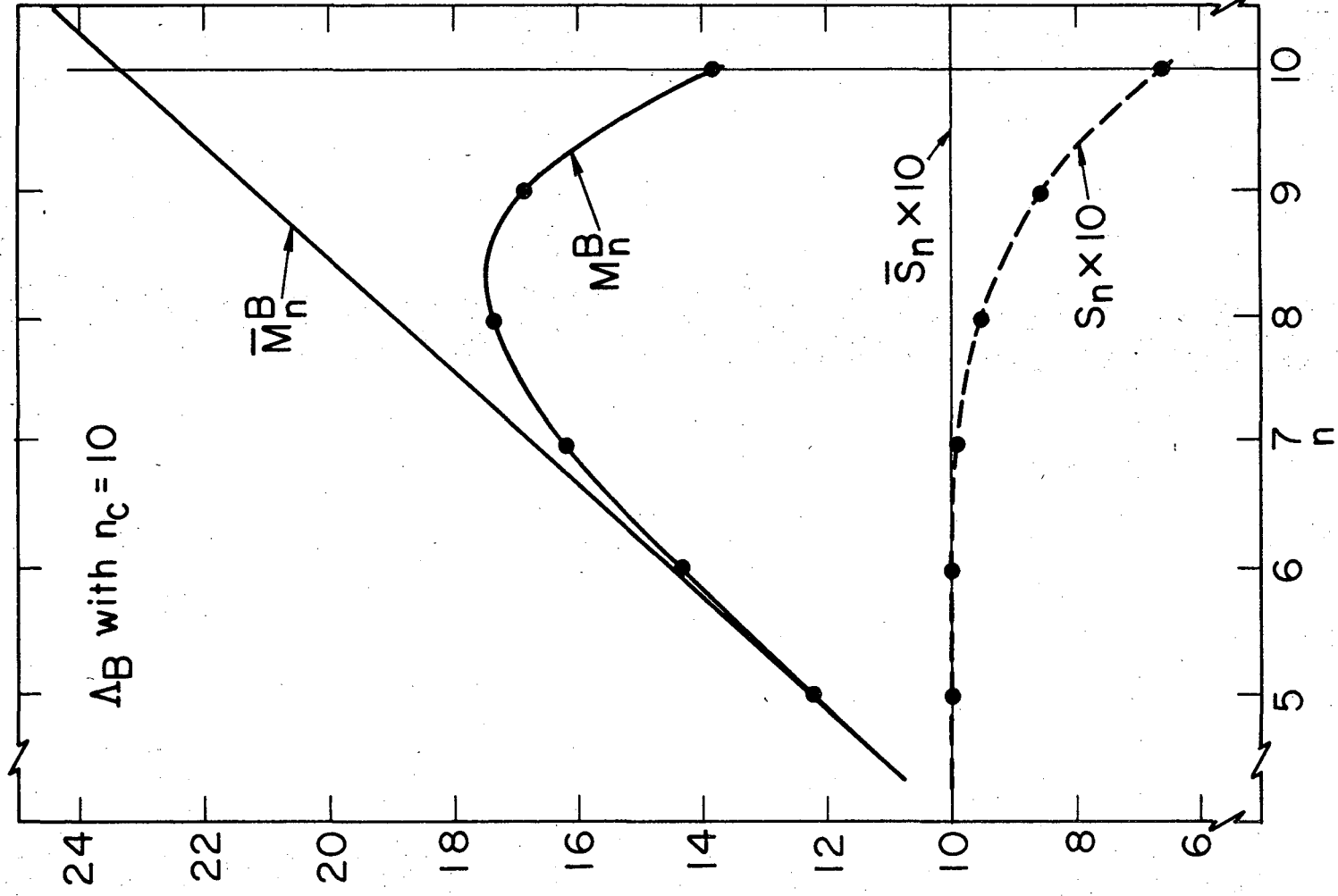
FIGURE CAPTIONS

- Fig. 1. The convergence of the M_{10}^{CO} integrations for the hydrogenic system. The angular integral in (3.8) is carried out using both the semianalytic method and the Newton-Cotes (5 point) integrations. The mesh size h is defined by $h = 2/K_{\max}$.
- Fig. 2. The values of M_n^B and S_n for the one-dimensional harmonic oscillator model are given near the cutoff $n_C = 10$, where the projection operator Λ_B is used.
- Fig. 3. The values of $M_n^{B\pm}$ and S_n^{\pm} for the one-dimensional harmonic oscillator model are given near the cutoff $n_C = 10$, where the projection operator Λ_B^{\pm} is used.
- Fig. 4. Variations in n of the exact dipole transition probabilities of the hydrogenic system for the processes $(n, \ell) \rightarrow$ (all states, with $\ell + 1$), \rightarrow (all bound states with $\ell + 1$), and \rightarrow (all continuum states with $\ell + 1$). The cases with $\ell = 0$ and 1 are considered.



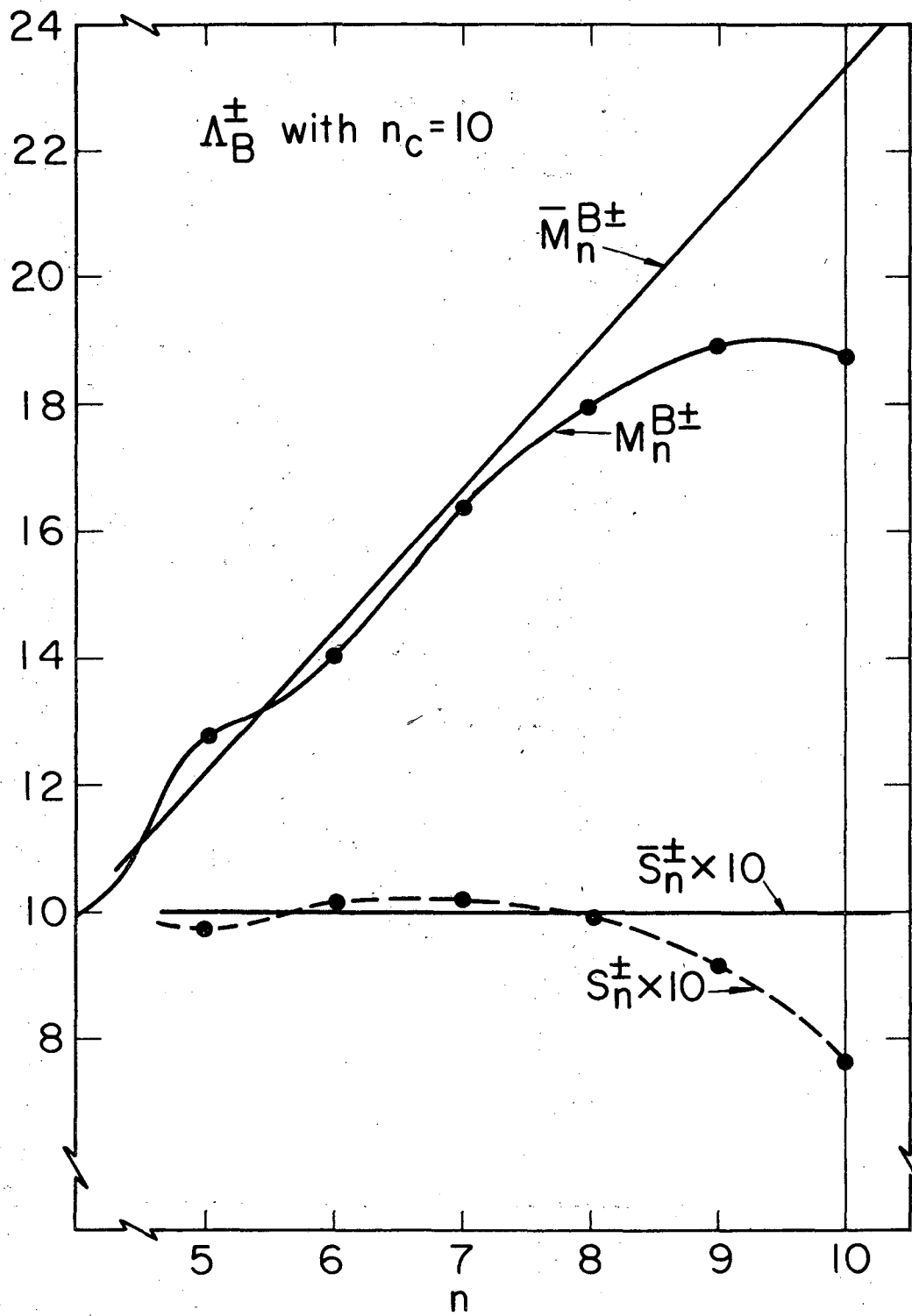
XBL 722-2321

Fig. 1



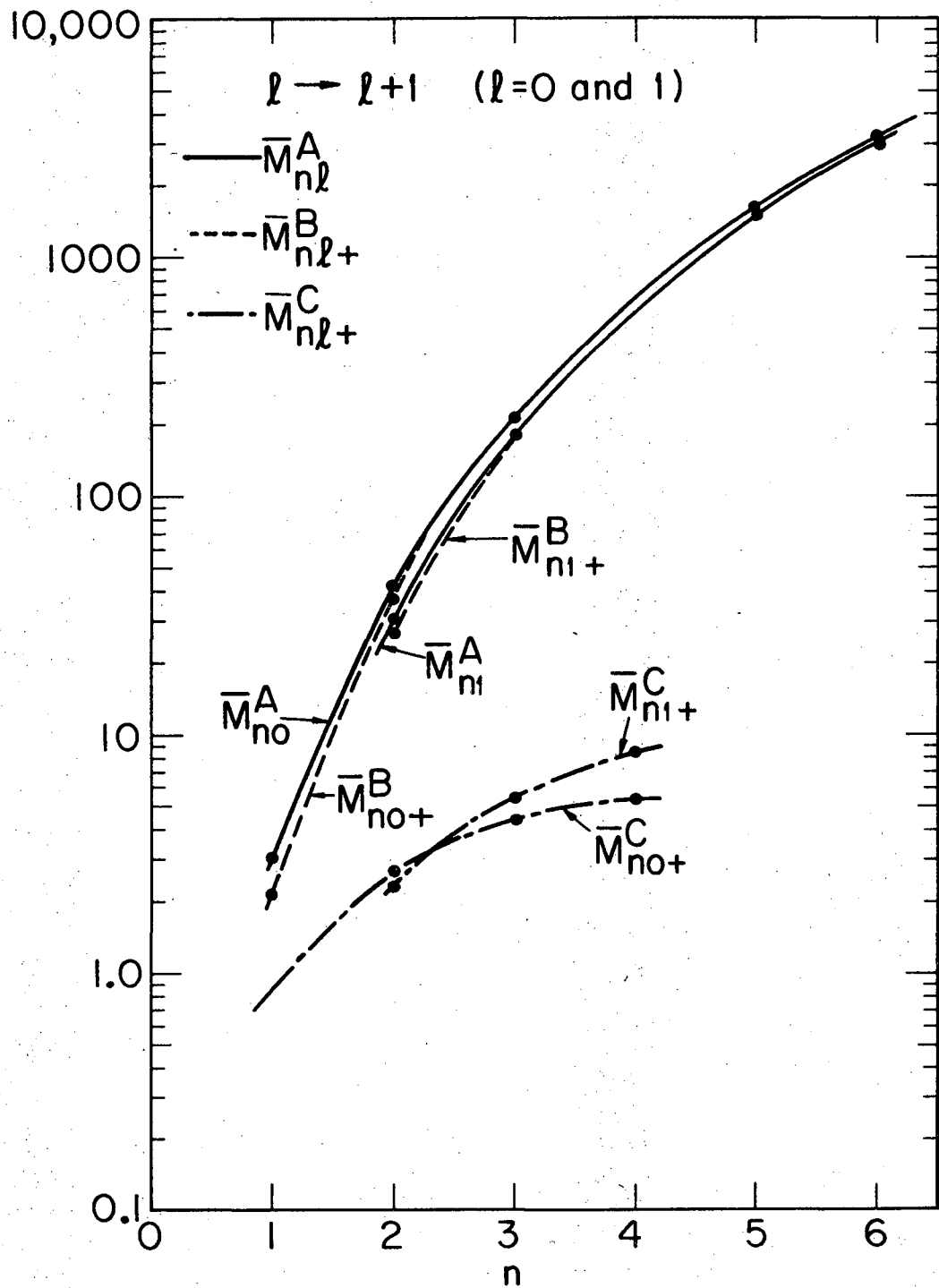
XBL 722 - 2320

Fig. 2



XBL722-2319

Fig. 3



XBL722 - 2318

Fig. 4

LEGAL NOTICE

This report was prepared as an account of work sponsored by the United States Government. Neither the United States nor the United States Atomic Energy Commission, nor any of their employees, nor any of their contractors, subcontractors, or their employees, makes any warranty, express or implied, or assumes any legal liability or responsibility for the accuracy, completeness or usefulness of any information, apparatus, product or process disclosed, or represents that its use would not infringe privately owned rights.

TECHNICAL INFORMATION DIVISION
LAWRENCE BERKELEY LABORATORY
UNIVERSITY OF CALIFORNIA
BERKELEY, CALIFORNIA 94720